RESEARCH ARTICLE | OCTOBER 01 1989

Highly excited rovibrational states using a discrete variable representation: The H^+_3 molecular ion

Jonathan Tennyson; James R. Henderson

J. Chem. Phys. 91, 3815–3825 (1989)
https://doi.org/10.1063/1.456867

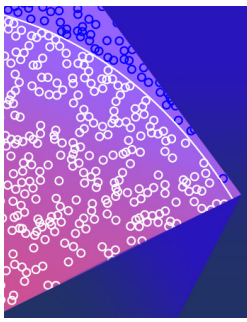

Highly excited rovibrational states using a discrete variable representation: The H_3^+ molecular ion

Jonathan Tennyson[a),b)]
Chemical Physics Department, Weizmann Institute of Science, 76100 Rehovot, Israel

James R. Henderson
Department of Physics and Astronomy, University College London, London WC1E 6BT, United Kingdom

(Received 17 May 1989; accepted 21 June 1989)

A formulation of the rovibrational problem in Jacobi coordinates is presented which employs a discrete variable representation for the angular internal coordinate. Rotational excitation is implemented via a two-step procedure and symmetry (for AB_2 systems) included using a computationally efficient method. Energies for the lowest 180 vibrational states of H_3^+ are presented and their wavefunctions analyzed graphically. $J = 1 \leftarrow 0$ excitation energies are presented for the lowest 41 vibrational states. The significance of the regular states in the high-energy regime of H_3^+ is discussed.

I. INTRODUCTION

The first-principles calculation of the low-lying rovibrational states of triatomic systems can now be routinely achieved by a number of methods,[1-3] and computer packages[4,5] exist for obtaining entire stick spectra. However, these methods, based on the use of basis set expansions and the variational principle rapidly become intractable if high-lying rovibrational states are required.

Recently, Bačić and co-workers[10] have developed methods of calculating vibrational wavefunctions using a discrete variable representation (DVR) in one or more coordinates. Their results are impressive, giving accurate energy levels for much higher vibrational states than had been previously achieved.

The quest for theoretical techniques to treat high-lying vibrational levels is timely for a number of reasons. Experiments using lasers can now probe these intermediate- and high-energy regions both by direct excitation and via electronically excited states of the system. Furthermore, high-lying rovibrational levels provide an important link between spectroscopy and reaction dynamics. An impressive example of this is the still unassigned near-dissociation, infrared spectra of H_3^+ obtained by Carrington and Kennedy.[11] They observed 27 000 lines in a small, 300 cm^{-1}, spectral region.

For a number of years Tennyson and Sutcliffe have worked on finite basis representations (FBR's) of molecular wavefunctions using body-fixed internal coordinates.[1,12-14] Using these methods and an accurate *ab initio* potential due to Meyer, Botschwina, and Burton (MBB),[15] Miller and Tennyson have performed a series[16-18] of highly accurate calculations of H_3^+ and its isotopomers. These have led to the first observation of the rotational spectrum of D_2H^+,[19] and to the assignment of both "hot" and overtone bands in H_3^+. These in turn lead directly to the assignment of an H_3^+ overtone emission spectrum in Jupiter.[20]

In this paper we report calculations incorporating the DVR of Bačić and Light[6,7] into our FBR programs[4] to yield an efficient method of calculating high-lying rovibrational levels of triatomic systems. We show how rotational excitation can be accounted for using the two-step variational technique of Tennyson and Sutcliffe,[14] and how the use of symmetry in a DVR can lead to greater computational savings than its use with the equivalent FBR.

Using this method and the MBB potential, we obtain converged eigenvalues and wavefunctions for the lowest 180 vibrational states of H_3^+, considerably extending the range studied by Whitnell and Light,[9] who obtained results for the lowest 60 levels and a further 20 nondegenerate, higher lying states. We also calculate rotationally excited states for many of these vibrational levels, the first time a fully coupled rovibrational calculation has been performed for anything but a few low-lying states.

II. THEORY

A. The discrete variable representation

The theory of DVR techniques has been well reviewed by Bačić and Light.[10] They show that a DVR for a particular coordinate is obtained by transforming the appropriate FBR Hamiltonian matrix elements. In the case that the FBR is a set of orthogonal polynomials, the DVR is obtained at the Gaussian quadrature points of these polynomials, appropriately weighted.

In this work we use body-fixed atom-diatom scattering (or Jacobi) coordinates. These coordinates represent the interaction of an atom A with a diatom BC. We define r_1 as the BC bondlength, r_2 the distance from A to the BC center of mass, and θ the angle between $\mathbf{r}_1$ and $\mathbf{r}_2$. In these coordinates it is natural to represent the angular motion using associated Legendre polynomials, $\Theta_{jk}(\theta)$.[21] In this case the resulting radial Hamiltonian is well known.[12]

[a)] Permanent address: Department of Physics and Astronomy, University College London, London WC1E 6BT, United Kingdom.
[b)] BITNET/EARN address JT at UKACRL.

 0021-9606/89/193815-11$02.10

$$\hat{H} = \delta_{jj}\delta_{k'k}\left[\frac{-\hbar^2}{2\mu_1}\frac{\partial^2}{\partial r_1^2} - \frac{\hbar^2}{2\mu_2}\frac{\partial^2}{\partial r_2^2} + \frac{\hbar^2}{2}j(j+1)\left(\frac{1}{\mu_1 r_1^2} + \frac{1}{\mu_2 r_2^2}\right) + \frac{\hbar^2}{2\mu_1 r_1^2}[J(J+1) - 2k^2]\right]$$
$$- \delta_{jj}\delta_{k'k\pm 1}(1 + \delta_{k0} + d_{k'0})^{1/2}\frac{\hbar^2}{2\mu_1 r_1^2}C_{jk}^{\pm}C_{jk}^{\pm} + \delta_{k'k}\langle j'k|V(r_1,r_2,\theta)|jk\rangle_\theta, \quad (1)$$

where the integral runs only over the angular coordinate. In (1) the reduced masses are given by

$$\mu_1 = \frac{m_B m_C}{m_B + m_C}, \quad \mu_2 = \frac{m_A(m_B m_C)}{m_A + m_B + m_C} \quad (2)$$

and

$$C_{jk}^{\pm} = [J(J+1) - k(k\pm 1)]^{1/2}. \quad (3)$$

The Hamiltonian (1) has the body-fixed z axis placed along the $\mathbf{r}_1$ direction. The Hamiltonian for z fixed along $\mathbf{r}_2$ is obtained simply by replacing $\mu_1 r_1^2$ by $\mu_2 r_2^2$ in terms involving J and k.[1]

In (1) only the Coriolis coupling term is off diagonal in k. In the two-step variational approach of Tennyson and Sutcliffe[14] the first step is to solve the Hamiltonian $\hat{H}^k$ obtained by assuming k is a good quantum number. The solutions of these "vibrational" problems are then used as a basis for the full, Coriolis-coupled Hamiltonian.

In this work we use the same approach to solve the second variational step but apply a DVR in the θ coordinate to solve the first step. If $\chi_k(=\cos\theta_k)$ and ω_k are the points and weights of N-point Gauss-associated Legendre quadrature, then a transformation for the $\hat{H}^k$ can be written

$$T_{j\alpha}^k = N_{jk}\omega_{k\alpha}^{1/2}\Theta_{jk}(\theta_{k\alpha}) = \omega_{k\alpha}^{1/2}|jk\rangle, \quad (4)$$

where N_{jk} normalizes Θ_{jk}. This transformation, for the $\mathbf{r}_1$ embedding, gives

$$H_{\alpha\alpha'}^k = \delta_{\alpha\alpha'}\left\{\frac{-\hbar^2}{2\mu_1}\frac{\partial^2}{\partial r_1^2} - \frac{\hbar^2}{2\mu_2}\frac{\partial^2}{\partial r_2^2} + \frac{\hbar^2}{2\mu_1 r_1^2}[J(J+1) - 2k^2] + V(r_1,r_2,\theta_{k\alpha})\right\}$$
$$+ \frac{\hbar^2}{2}\left(\frac{1}{\mu_1 r_1^2} + \frac{1}{\mu_2 r_2^2}\right)L_{\alpha\alpha'}^k, \quad (5)$$

where

$$L_{\alpha\alpha'}^k = \sum_{j=k}^{N+k-1} T_{j\alpha'}^k j(j+1) T_{j\alpha}^k. \quad (6)$$

The Hamiltonian $\hat{H}_{\alpha\alpha'}^k$, can be compactly expressed in matrix notation as

$$\hat{\mathbf{H}}^k = \hat{\mathbf{h}}^k(r_1,r_2)\mathbf{I} + w(r_1,r_2)\mathbf{L}^k. \quad (7)$$

In deriving $\hat{H}_{\alpha\alpha'}^k$, the approximation

$$\sum_{jj'=k}^{N+k-1} T_{j\alpha}^k \langle j'k|V(r_1,r_2,\theta)|jk\rangle_\theta T_{j\alpha}^k \simeq \delta_{\alpha\alpha'}V(r_1,r_2,\theta_{k\alpha}), \quad (8)$$

which is equivalent to the N-point Gauss-associated Legendre quadrature,[22] has been assumed. Solving this problem is equivalent to using an FBR including all Θ_{jk} up to $j = N + k - 1$.

The solution strategy is to then solve the two-dimensional Hamiltonian, $\hat{h}_\alpha^k$, for each α and to use these solutions to solve the $\hat{\mathbf{H}}^k$. The advantage of this technique is that not all solutions of the $\hat{h}^k$ are needed to converge the lower-lying solutions of $\hat{\mathbf{H}}^k$. This leads to large savings in the size of the final secular matrix that needs to be diagonalized.

The coupling between α blocks is provided by the angular kinetic energy term as expressed by the term involving the L matrix. Of course there is some flexibility in how one defines the two-dimensional (2D) Hamiltonian. In particular, one can either include terms diagonal in L in either the 2D or 3D problem. For reasons which will become apparent we prefer the second option.

Finally, for calculations with $J > 0$, the lowest M solutions of the $\hat{\mathbf{H}}^k$ are used to expand the fully Coriolis-coupled Hamiltonian.[14,23] This part of the calculation is performed by program ROTLEVD,[4] which was originally designed to be driven by an FBR program TRIATOM.

B. Wave functions

In this work a finite basis representation (FBR) is used to expand the solutions of the 2D Hamiltonian, $\hat{h}_\alpha^k$. The rth wave function, with eigenenergy $\epsilon_{\alpha r}^k$, can then be written

$$\phi_{\alpha r}^{Jk}(r_1,r_2;\theta_{k\alpha}) = \sum_{m,n} a_{mn\alpha}^{Jkr} H_m(r_1) H'_n(r_2) D_{Mk}^J(\Omega). \quad (9)$$

For the radial functions, H_m and H'_n, we use orthogonal polynomials based on the solutions of model potentials such as the Morse or spherical oscillator problems.[1]

Solutions of Hamiltonian $\hat{\mathbf{H}}^k$ are then expressed in terms of the $\boldsymbol{\phi}^{Jk}$:

$$\Psi_s^{Jk}(r_1,r_2,\theta_{k\alpha}) = \sum_r b_{\alpha r}^{Jks}\phi_{\alpha r}^{Jk}$$
$$= \sum_{m,n} c_{mn\alpha}^{Jks} H_m(r_1) H'_n(r_2) D_{Mk}^J(\Omega), \quad (10)$$

where

$$c_{mn\alpha}^{Jks} = \sum_r a_{mn\alpha}^{Jkr} b_{\alpha r}^{Jks}. \quad (11)$$

For the second variational step it is desirable to have wave functions expressed in an FBR expansion. This is because the off-diagonal Coriolis coupling terms, in Jacobi coordinates, are diagonal in j but off diagonal in α. So writing

$$\Psi_s^{Jk}(r_1,r_2,\theta) = \sum_{j,m,n} d_{jmn}^{Jks} H_m(r_1) H'_n(r_2)\Theta_{Jk}(\theta) D_{Mk}^J(\Omega), \quad (12)$$

one obtains the coefficients of the FBR by backtransforming

$$d_{jmn}^{Jks} = \sum_\alpha T_{\alpha j}^k c_{mn\alpha}^{Jks} = \sum_\alpha N_{jk}\omega_{k\alpha}^{1/2}\Theta_{jk}(\theta_{k\alpha}) c_{mn\alpha}^{Jks}. \quad (13)$$

As $\hat{\mathbf{H}}^k$ depends only on k^2, the d^{Jks} depend only on $|k|$. The d^{Jks} form the input for the second variational step yielding a final ro-vibrational wave function:

$$\Psi_t^{Jp}(r_1,r_2,\theta) = \delta_{k0}\delta_{p0}\sum_s e_{ks}^{Jpt}\psi_s^{Jk} + \sum_{k=1}^{J}\sum_s e_{ks}^{Jpt}2^{-1/2}[\psi_s^{Jk} + (-1)^p\psi_s^{J-k}]$$

$$= \delta_{k0}\delta_{p0}\sum_{jkmn} f_{jmn}^{Jpt}H_m(r_1)H'_n(r_2)\Theta_{jk}(\theta)D^J_{Mk}(\Omega)$$

$$+ \sum_{k=1}^{J}\sum_s f_{jkmn}^{Jpt}H_m(r_1)H'_n(r_2)2^{-1/2}[\Theta_{jk}(\theta)D^J_{Mk}(\Omega) + (-1)^p\Theta_{j-k}(\theta)D^J_{M-k}(\Omega)], \quad (14)$$

where

$$f_{jkmn}^{Jpt} = \sum_s d_{jmn}^{Jks}\, e_{ks}^{Jpt} \quad (15)$$

and p equals 0 or 1. The total parity of the wave function is given by $(-1)^{J+p}$.

C. Symmetry

The inclusion of symmetry in a DVR calculation has been the subject of a recent study by Whitnell and Light.[8] In this subsection we propose a slightly different, and computationally more efficient, procedure for symmetry adapting our DVR calculations.

In an FBR the symmetry of an AB_2 system is carried naturally by associated Legendre polynomials. Functions with j even are symmetric and those with j odd antisymmetric with respect to reflection about $\theta = 90°$. In this case the symmetry of the Gauss-associated Legendre quadrature about $\chi = \cos\theta = 0$ means that all the unique problems lie in the half range $0 \leqslant \chi_{k\alpha} < 1$. It is then possible to symmetrize the DVR wave function $\phi_{\alpha r}^{Jk}$ by writing

$$\phi_{\alpha r}^{Jkq}(r_1,r_2;\chi_{k\alpha}) = 2^{-1/2}[\phi_{\alpha r}^{Jk}(r_1,r_2;\theta_{k\alpha}) + (-1)^q\phi_{\alpha r}^{Jk}(r_1,r_2;\pi/2-\theta_{k\alpha})],$$
$$q = 0,1, \quad \chi_{k\alpha} > 0, \quad (16)$$

where we have restricted ourselves to an even number of DVR points, N, to avoid the special case of $\chi_{k\alpha} = 0$.

Transforming $\hat{H}^k_{\alpha\alpha'}$ to this symmetrized basis gives

$$\hat{\mathbf{H}}^{kq} = \hat{\mathbf{h}}^k\mathbf{I} + w(r_1,r_2)\mathbf{L}^{kq}, \quad (17)$$

where

$$L^{kq}_{\alpha\alpha'} = 2\sum_{l=k}^{N/2+k-1} T^k_{2l+q,\alpha'}(2l+q)(2l+q+1)T^k_{2l+q,\alpha}. \quad (18)$$

This means that in the symmetrized DVR only the term which differs between even ($q = 0$) and odd ($q = 1$) calculations is provided by the $\mathbf{L}^{kq}$ matrix.

The matrix elements of $\hat{H}^{kq}$ can be expressed as

$$\langle\alpha' r'|\hat{H}^{kq}|\alpha r\rangle = \delta_{\alpha\alpha'}\delta_{rr'}\epsilon^k_{\alpha r} + \tilde{W}_{\alpha' r'\alpha r}L^{kq}_{\alpha'\alpha} \quad (19)$$

where

$$\tilde{W}_{\alpha' r'\alpha r} = \sum_{m,n}\sum_{m',n'} a^{Jkr}_{mn\alpha}a^{Jkr'}_{m'n'\alpha'}\langle m'n'|w(r_1,r_2)|mn\rangle. \quad (20)$$

The orthogonal coordinates used here simplify this transformation as

$$\langle m'n'|w(r_1,r_2)|mn\rangle = \delta_{nn'}\langle m'|\frac{\hbar^2}{2\mu_1 r_1^2}|m\rangle + \delta_{mm'}\langle n'|\frac{\hbar^2}{2\mu_2 r_2^2}|n\rangle. \quad (21)$$

The transformation step is still found to dominate the CPU time requirement.

The advantage of our method of symmetrization is now clear. Not only do we solve on a reduced DVR grid for a given symmetry block, but also if both symmetry blocks are required the results for the second can be computed at relatively small cost. Doing this requires simply saving the eigenvalues and eigenvectors of the $\hat{h}^k_\alpha$ and the transformed matrix $\tilde{\mathbf{W}}$.

III. CALCULATIONS ON H_3^+

A. $J=0$

In a recent study of near dissociating states of H_3^+, Tennyson, Brass and Pollak[24] (TBP) performed a series of reduced dimensionality calculations on the system in the C_{2v} subspace obtained by freezing θ at 90°. By using basis sets composed of 23 Morse oscillator-like functions for the r_1 coordinate and 29 spherical oscillators for the r_2 coordinate, they were able to obtain converged solutions for the system up to dissociation. These calculations correspond closely to the first step in the DVR approach outlined here and involve simply the solution of $\hat{h}^k_\alpha$ for $\chi_{k\alpha} = 0$.

Test calculations at other angles showed that TBP's basis was flexible enough to give a good representation of the system for a range of θ values. It was therefore decided to use this basis to represent the solutions of $\hat{h}^k_\alpha$.

Table I shows the convergence characteristics of a selection of states as a function of changing the size of final basis, and DVR grid, N. Demonstrating convergence with the DVR method is not as straightforward as with FBR calculations. This is first because the DVR method is not variational, and therefore convergence is not necessarily obtained from above, and second because increasing the DVR grid can make a calculation worse unless some means is devised to keep the number of functions per grid point approximately constant.

The method employed by Bačić and Light[6] to solve the second problem is to include all functions in the final problem whose eigenenergies, $\epsilon^k_{\alpha r}$, lie below some energy cutoff, $\epsilon^{\max}$. The first three columns of Table I demonstrate the effect of increasing the number of DVR points with a constant cutoff energy. The final columns show convergence for a constant grid as the energy cutoff or total number of functions included in the final problem, L, is increased.

TABLE I. H_3^+ vibrational band origins, in cm^{-1}, as a function of DVR points, N, size of the final Hamiltonian matrix, L, and cutoff energy, in cm^{-1}, relative to the lowest 2D solution, ϵ^{max}.

	1	2	3	4	5
L	2000	2222	2657	2400	2800
N	36	40	48	36	36
ϵ^{max}	34 930	34 930	34 930	37 390	39 669
Level	1	2	3	4	5
21	10 592.6	10 592.6	10 592.6	10 592.4	10 592.3
41	13 582.1	13 582.1	13 582.1	13 581.3	13 580.9
61	15 369.8	15 369.9	15 370.0	15 368.9	15 368.3
81	17 219.1	17 219.1	17 219.2	17 217.7	17 217.0
101	18 435.0	18 435.1	18 435.1	18 433.7	18 433.1
121	19 514	19 514	19 514	19 511	19 509
141	20 498	20 498	20 498	20 495	20 493
161	21 433	21 433	21 434	21 429	21 428
180	22 215	22 215	22 215	22 209	22 206

The final column of Table I gives our best results which are presented in full in Table II. For E symmetry states only the lower component of each doublet is shown. For comparison the results of Whitnell and Light[9] (WL) and Miller and Tennyson[18] are also given. Assignments are also given where possible. These assignments were obtained by plotting cuts through the wave functions for $\theta = 90°$ and confirmed by inspecting other cuts with $\theta = 80°$, 70°, and 0°. This method of assignment is necessarily approximate and was only attempted for even $q = 0$ (A_1 or E_e) states as the odd $q = 1$ (A_2 or E_o) states have a node at $\theta = 90°$. The assignment of a vibrational angular momentum quantum number, l, to excitations of the degenerate ν_2 bending mode is not possible by visual inspection of the plots and has not been attempted.

B. $J=1$

Calculations for the first rotationally excited state of H_3^+ were performed using the $N = 36$, $L = 2800$ basis used for the $J = 0$ results presented in Table I. Table III shows the convergence of the lowest 151 $J = 1, p = 0, q = 0$ states as a function of the number of functions, M, included in the final step of the calculation. The levels span the rotational manifold of the lowest 102 vibrational states.

Table IV gives all the $J = 1$ levels of H_3^+ for the lowest vibrational states. The results are only presented in this form for the lowest 41 states as analysis of the higher states becomes increasingly difficult. This is because the increased density of states makes the assignment of rotational levels to a particular vibrational state on energy criteria rather arbitrary. However, we should also note that in this region several "degenerate" states began to show large splittings. These splittings were significantly larger than both those in the corresponding $J = 0$ calculations and the convergence suggested by Table III. Analysis of the states showing large splittings clearly indicates that they are associated with states with appreciable amplitude at linear geometries and in particular the so-called "horseshoe" states (see below). The onset of this behavior appears very suddenly in our results.

In Table IV no attempt has been made to assign quantum numbers to the rotational levels beyond symmetry designations. Watson[25] has suggested means of quantizing and parametrizing the rotational levels of X_3 systems. However, such schemes are only appropriate for molecules undergoing small-amplitude vibrational motion. This is clearly not the case for the majority of states considered here.

Table IV also gives a comparison with the FBR results of Miller and Tennyson,[17] where a detailed comparison with experiment can also be found. Our results are in very good agreement with this study. Finally, we note that Table IV includes results for A_1 states of H_3^+ which are forbidden by nuclear-spin statistics. These results have been included as they yield useful data about the rotational structure of the system and can be compared with the results of other calculations.

IV. DISCUSSION

In appraising the validity of our results, it is important to have an assessment of convergence. This can be obtained by comparing results as a function of the parameters of the calculation, samples of which are presented in Tables I and III and also by monitoring the splitting between degenerate states. These tests suggest that the lowest 63 vibrational levels presented in Table II are converged to 1 cm^{-1}, the lowest 148 states to 5 cm^{-1} and the remainder to 10 cm^{-1}. Indeed there is evidence that more vibrational states than the 180 presented here are converged to 10 cm^{-1}, but the MBB potential employed in these calculations is only valid up to 25 000 cm^{-1} above the minimum.[15] Therefore there seems to be little reason for analyzing states much beyond this point.

For the states common to both studies, our convergence is similar to that claimed by WL.[9] However, comparison of the results shows that our results are consistently lower. A small systematic difference of approximately 1 cm^{-1} was known previously and is believed to be due to the slightly less accurate constants employed by WL, but there are also very much larger discrepancies for the higher states. These discrepancies vary greatly from level to level and in many cases

TABLE II. Band origins, in cm^{-1}, for the lowest 180 states of H_3^+ calculated using $L = 2800$, $N = 36$. Results due to Whitnell and Light (WL) and Miller and Tennyson (MT) are shown for comparison. Tentative assignments are given where possible.

Level	Symmetry	$(v_1,v_2^l)^a$	This work	WL[b]	MT[c]
1	A_1	$(0,0^0)$	[4363.5][d]	[4364.0][d]	[4363.5][d]
2	E	$(0,1^1)$	2521.3	2521.5	2521.3
3	A_1	$(1,0^0)$	3178.4	3178.7	3178.4
4	A_1	$(0,2^0)$	4777.1	4777.5	4777.0
5	E	$(0,2^2)$	4997.4	4997.6	4997.4
6	E	$(1,1^1)$	5553.7	5554.2	5553.7
7	A_1	$(2,0^0)$	6262.0	6262.6	6262.0
8	E	$(0,3^1)$	7003.5	7003.9	7003.4
9	A_1	$(0,3^3)$	7282.6	7283.2	7282.5
10	A_2	$(0,3^3)$	7492.7	7493.3	7492.7
11	A_1	$(1,2^0)$	7769.2	7770.0	7769.2
12	E	$(1,2^2)$	7868.7	7869.1	7868.8
13	E	$(2,1^1)$	8487.0	8487.7	8487.1
14	A_1	$(0,4^0)$	8996.8	8997.6	
15	E	$(0,4^2)$	9107.7	9108.2	
16	A_1	(3,0)	9251.6	9252.6	9251.6
17	E	(1,3)?	9650.7	9651.1	
18	A_1	(1,3)	9964.2	9965.0	
19	E	(1,3)?	9996.6	9997.5	
20	A_2		10 208.6	10 209.5	
21	A_1	(2,2)?	10 592.3	10 593.3	
22	E	(2,2)?	10 642.8	10 643.3	
23	E	(0,5)	10 853.5	10 854.1	
24	A_1	(0,5)	10 913.4	10 914.4	
25	E	(3,1)	11 321.6	11 322.5	
26	A_2		11 525.8	11.526.4	
27	E	(1,4)?	11 651.4	11 652.6	
28	A_1	(1,4)?	11 809.6	11 811.0	
29	E	u	12 073.5	12 074.2	
30	A_1	(4,0)	12 146.0	12 417.4	
31	E	(0,6)	12 294.5	12 295.5	
32	A_1	(0,6)	12 363.8	12 365.2	
33	E	(0,6)?	12 467.8	12 469.0	
34	A_1	(2,3)?	12 584.7	12 585.8	
35	E	(2,3)?	12 694.3	12 695.8	
36	A_2		12 828.6	12 829.5	
37	A_1	u	13 285.1	13 286.8	
38	E	(4,1)?	13 313.7	13 314.9	
39	E	(1,5)?	13 385.6	13 387.6	
40	A_1	(1,4)?	13 392.2	13 395.6	
41	E	(1,5)?	13 581.0	13 582.7	
42	E	(0,7)	13 681.3	13 684.7	
43	A_1	(0,7)?	13 706.0	13 708.3	
44	A_2		13 747.3	13 747.9	
45	E	(4,1)	14 052.5	14 053.4	
46	A_1	u	14 186.1	14 191.6	
47	E	(2,4)?	14 211.5	14 216.7	
48	E	(2,4)?	14 465.2	14 471.7	
49	A_2		14 564.4	14 566.2	
50	A_1	(2,4)?	14 663.4	14 666.6	
51	E	(1,6)?	14 878.7	14 888.6	
52	A_1	u	14 886.2	14 902.9	
53	E	u	14 886.4	14 890.9	
54	A_1	(5,0)	14 939.0	14 940.9	
55	A_1	(0,8)?	15 062.0	15 067.1	
56	E	(0,8)	15 103.8	15 108.3	
57	A_1	u	15 158.3	15 160.3	
58	A_2		15 179.1	15 180.1	
59	E	(3,3)?	15 203.3	15 206.3	
60	E	(3,3)?	15 325.2	15 332.0	
61	A_2		15 368.3	15 369.6	
62	E	u	15 772.0		
63	A_1	u	15 868.5	15 878.2	
64	E	(5,1)?	15 881.6		
65	A_1	u	15 909.3	15 936.4	
66	A_2		15 952.0	15 955.1	
67	E	(2,5)?	16 006.6		

TABLE II (*continued*).

Level	Symmetry	(v_1,v_2^l)[a]	This work	WL[b]	MT[c]
68	A_1	(1,7)?	16 195.6	16 223.3	
69	E	(1,7)?	16 243.8		
70	E	u	16 442.9		
71	A_1	u	16 444.2	16 457.4	
72	E	u	16 546.3		
73	A_2		16 580.7	16 583.3	
74	E	(5,1)?	16 667.3		
75	A_1	(0,9)	16 695.6	16 706.2	
76	E	(0,9)?	16 713.2		
77	E	u	16 859.3		
78	E	u	16 910.5		
79	A_1	u	17 061.4	17 118.1	
80	A_2		17 078.7	17 084.6	
81	E	u	17 217.0		
82	A_1	u	17 273.9	17 332.7	
83	E	(2,6)?	17 386.6		
84	A_1	u	17 429.2	17 459.6	
85	E	u	17 440.8		
86	A_1	(6,0)	17 586.1	17 588.6	
87	E	u	17 601.7		
88	A_2		17 672.3	17 688.0	
89	A_1	(6,0)	17 681.0	17 689.5	
90	E	u	17 692.3		
91	A_1	(1,8)?	17 746.3	17 779.9	
92	A_2		17 809.5	17 826.6	
93	E	u	17 847.2		
94	A_2		17 858.1	17 856.5	
95	E	u	17 957.4		
96	E	u	18 210.3		
97	A_1	u	18 226.6	18 353.7	
98	A_2		18 319.6	18 328.6	
99	E	12[e]	18 346.4		
100	A_1	u	18 360.8		
101	E	(0,10)	18 433.1		
102	A_1	(0,10)?	18 456.8		
103	E	u	18 568.1		
104	A_1	u	18 584.2		
105	E	(2,7)?	18 711.4		
106	A_1	u	18 794.6		
107	E	u	18 795.7		
108	A_2		18 869.4	18 911.3	
109	E	13?[e]	18 915.3		
110	E	13?[e]	19 039.0		
111	E	(1,9)?	19 079.5		
112	A_1	(2,8)?	19 098.5		
113	A_2		19 180.0	19 197.3	
114	E	(2,8)?	19 209		
115	E	13?[e]	19 255		
116	E	u	19 272		
117	A_1	u	19 300		
118	A_2		19 301	19 335.6	
119	E	u	19 411		
120	A_1	u	19 414		
121	E	u	19 509		
122	A_2		19 726		
123	E	u	19 754		
124	A_1	u	19 761		
125	A_1	u	19 805		
126	E	u	19 828		
127	E	u	19 863		
128	E	u	20 047		
129	A_2		20 048		
130	A_1	14[e]	20 068		
131	E	(2,8)?	20 091		
132	A_1	(0,11)?	20 178		
133	A_1	(7,0)?	20 206		
134	E	(0,11)?	20 211		
135	E	(0,11)	20 241		

TABLE II (*continued*).

Level	Symmetry	$(v_1,v_2^l)^a$	This work	WL[b]	MT[c]
136	A_2		20 277		
137	A_1	u	20 336		
138	A_2		20 362		
139	E	u	20 426		
140	A_1	u	20 490		
141	E	u	20 493		
142	E	u	20 596		
143	A_1	u	20 613		
144	A_1	u	20 764		
145	A_2		20 771		
146	E	u	20 777		
147	A_2		20 814		
148	A_1	u	20 832		
149	E	(1,10)	20 854		
150	E	u	20 925		
151	E	u	20 974		
152	A_1	u	21 026		
153	E	u	21 106		
154	E	u	21 144		
155	A_2		21 179		
156	A_1	u	21 206		
157	A_1	u	21 220		
158	E	u	21 265		
159	E	u	21 311		
160	A_2		21 330		
161	E	u	21 428		
162	A_1	u	21 465		
163	E	u	21 539		
164	A_2		21 585		
165	E	u	21 591		
166	A_1	(2,9)?	21 629		
167	E	15?[e]	21 663		
168	E	u	21 666		
169	A_1	u	21 728		
170	E	u	21 762		
171	E	u	21 884		
172	A_2		21 892		
173	E	u	21 899		
174	A_1	15?[e]	21 992		
175	A_1	u	22 087		
176	E	(0,12)?	22 120		
177	A_2		22 144		
178	E	u	22 161		
179	A_1	(0,12)	22 176		
180	E	(0,12)?	22 206		

[a]? denotes states with distorted model structures. u denotes states that could not be assigned.
[b]Reference 9.
[c]Reference 18.
[d]Zero-point energy.
[e]States assigned to the "inverted hyperspherical mode" (Ref. 24).

TABLE III. Convergence of H_3^+ $J=1, p=0, q=0$ levels as a function of dimension of the final Hamiltonian, M. Frequencies, in cm^{-1} are relative to the $J=0$ ground state.

Level	$M=200$	$M=600$	$M=900$	$M=1200$
1	64.11	64.11	64.11	64.11
16	7 876.07	7 875.94	7 875.94	7 875.94
31	10 659.40	10 658.96	10 658.95	10 658.94
46	12 381.25	12 379.49	12 379.46	12 379.45
61	13 722.25	13 718.37	13 718.21	13 718.16
76	14 939.1	14 930.8	14 930.6	14 930.6
91	15 912.1	15 895.2	15 893.9	15 893.3
106	16 714.8	16 699.1	16 698.0	16 697.6
121	17 494.9	17 465.0	17 463.3	17 462.5
136	18 073.7	17 981.9	17 968.4	17 962.5
151	18 743.4	18 671.6	18 669.2	18 668.4

are more than 20 cm^{-1}. Furthermore, states with A_2 symmetry appear, in general, to be in better agreement than states with A_1 or E symmetry. It is our belief that these discrepancies are caused by incomplete convergence in WL's calculations.

Nonetheless, comparison with WL's calculations was useful for us. This is because they use the full S_3 symmetry of the H_3^+ system and thus obtained unique symmetry assignments. Our calculations were performed in S_2 symmetry which means that an A_1 /A_2 pair which is degenerate to within our convergence limits is indistinguishable from a single-E symmetry state. This consideration must be borne in mind when analyzing the symmetry assignments to our higher states. In particular, states numbered 117 and 118 would have been assigned as a single-E state if it had not been for

TABLE IV. H_3^+ $J = 1 \leftarrow 0$ rotational frequencies in cm^{-1} and symmetry calculated using $L = 2800$, $N = 36$, $M = 1200$. Results due to Miller and Tennyson are shown for comparison.

$J=0$			$J=1$	
Level	Symmetry	Band origin	$p=0$	$p=1$
1	A_1	0.0	E, 64.11	A_2, 86.93
			64.10[a]	86.93[a]
2	E	2521.3	E, 26.76; A_2, 95.21; A_1, 105.90	E, 88.10
			26.76,[a] 95.21,[a] 105.90[a]	88.09[a]
3	A_1	3178.4	E, 62.47	A_2, 84.84
			62.47[b]	84.84[a]
4	A_1	4777.1	E, 64.18	A_2, 91.93
			64.1/64.2[a]	91.8
5	E	4997.4	A_2, −3.13; A_1, 0.98, E, 127.06	E, 89.53
			−3.2,[a] 1.0,[a] 127.0[a]	89.6/89.3[a]
6	E	5553.7	E, 30.05; A_2, 90.34; A_1, 100.01	E, 86.20
			30.0,[a] 90.3,[a] 100.0[a]	85.9/86.3[a]
7	A_1	6262.0	E, 60.91	A_2, 82.90
			60.9/60.8[a]	82.8[a]
8	E	7003.5	E, 40.74; A_2, 76.73; A_1, 103.91	E, 96.86
9	A_1	7282.6	E, 40.15	A_2, 82.90
10	A_2	7492.7	E, 78.45	A_1, 89.03
11	A_1	7769.2	E,70.79	A_2, 88.63
12	E	7868.7	A_2, 2.48; A_1, 7.22; E, 118.96	E, 88.49
13	E	8487.0	E, 31.89; A_2, 81.14; A_1, 95.45	E, 84.64
14	A_1	8996.8	E, 67.41	A_2, 107.86
15	E	9107.7	A_2, 25.34; A_1, 57.07; E, 98.48	E, 108.84
16	A_1	9251.6	E, 66.67	E, 88.47
17	E	9650.7	E, 25.27; A_2, 95.39; A_1, 146.03	E, 91.73
18	A_1	9964.2	E, 25.09[c]	A_2, 97.97
19	E	9996.6	E, 18.63[c]; A_2, 133.45; A_1, 146.03	E, 91.73
20	A_2	10 208.6	E, 71.29	A_1, 88.48
21	A_1	10 592.3	E, 66.67	A_2, 88.47
22	E	10 642.8	A_2, 10.17; A_1, 15.71; E, 109.90	E, 88.65
23	E	10 853.5	E, 56.1; A_2, 60.7; A_1, 137.5	E, 141.4
24	A_1	10 913.4	E, 104.2	A_2, 145.9
25	E	11 321.6	E, 33.7; A_2, 81.8; A_1, 91.4	E, 83.6
26	A_2	11 525.8	E, 63.4	A_1, 101.1
27	E	11 651.4	A_2, 35.7; A_1, 62.4; E, 88.9	E, 113.9
28	A_1	11 809.6	E, 75.1	A_2, 107.6
29	E	12 073.5	A_2, 27.4; A_1, 39.1; E, 69.8	E, 103.4
30	A_1	12 146.0	E, 58.0	A_2, 79.8
31	E	12 294.5	A_2, 40; A_1, 82; E, 85	E, 140
32	A_1	12 363.8	E, 132	A_2, 249
33	E	12 467.8	A_2, 44; E, 156; A_1, 181	E, 210
34	A_1	12 584.7	E, 98	A_2, 124
35	E	12 694.3	E, 28; A_2, 113; A_1, 145	E, 110
36	A_2	12 828.6	E, 67	A_1, 89
37	A_1	13 285.1	E, 66	A_2, 96
38	E	13 313.7	A_2, 21; A_1, 29; E, 97	E, 92
39	E	13 385.6	A_2, 49; A_1, 72; E, 81	E, 139
40	A_1	13 392.2	E, 119	A_1, 133
41	E	13 581.0	E, 72; A_2, 95; A_1, 137	E, 147

[a] Reference 17.
[b] This level is misprinted in Ref. 17.
[c] These states are nearly degenerate.

WL's prediction of an A_2 state in this region.

Table II also presents approximate assignments, where possible, to the 151 $q = 0$ states. Figures 1 and 2 present illustrative contour plots for eight of these states. While it is apparent that the majority of the states in the high-energy region are highly irregular in structure, there are some states which are spatially localized and for which assignments are possible. Noteworthy amongst these are regular states corresponding to highly-excited bending states; see Fig. 1, state 101. These states also exist with low degrees of stretching excitation; see state 148 of Fig. 2 for example.

Orbits of this nature were originally found by Berblinger, Pollak, and Schlier[26] using classical mechanics. These workers studied the phase-space structure of H_3^+ and found these horseshoe states (so named because of their shape if they are plotted with r_2 ranging from $-\infty$ to $+\infty$) were the only stable quasiperiodic orbits to occupy a significant portion of phase space at higher energies. How-

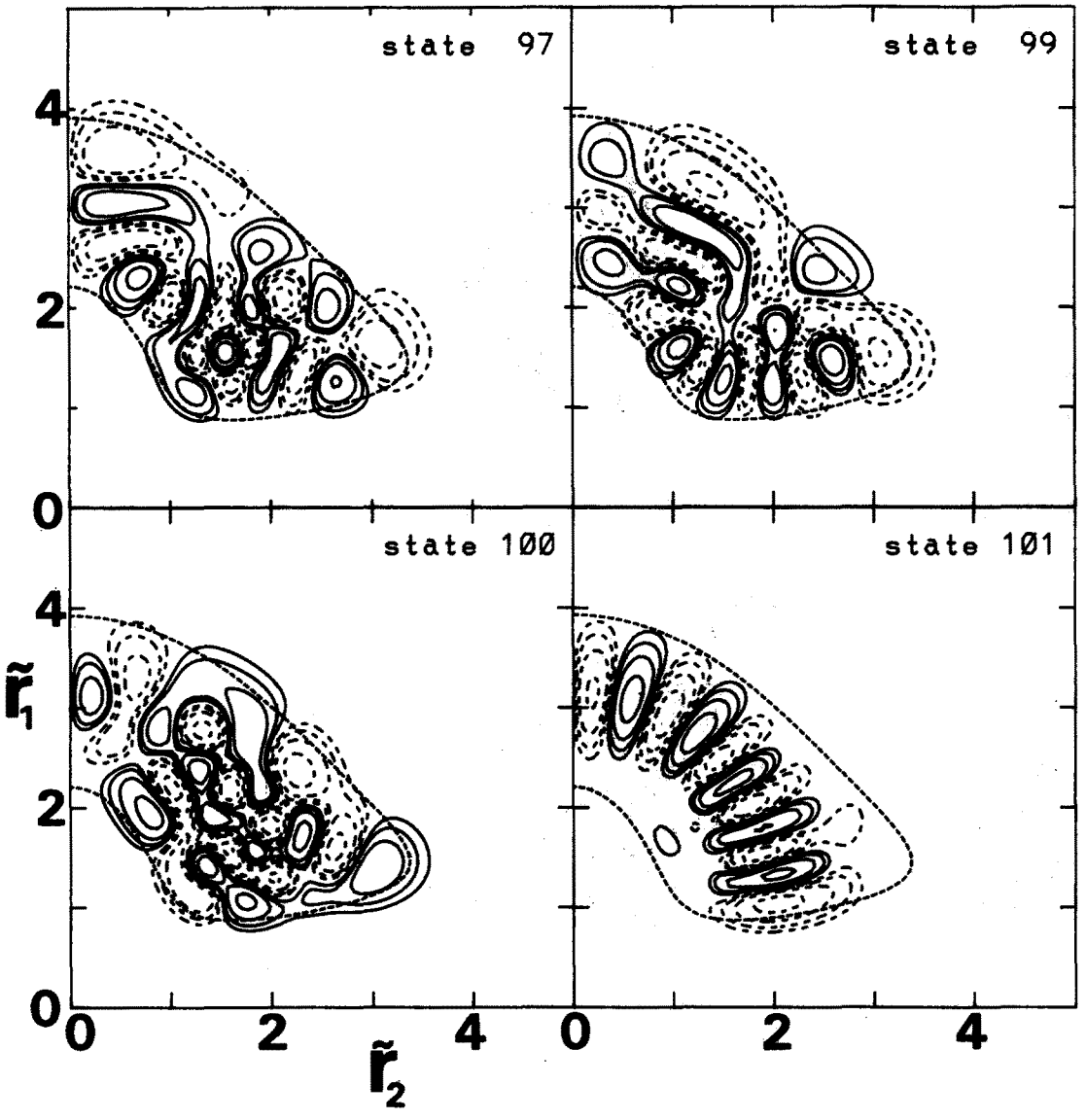

FIG. 1. Cuts through the wave function of four even $J = 0$ states with $\theta = 90°$. Contours are for 64%, 32%, 16%, and 8% of the maximum amplitude with solid (dashed) curves enclosing regions of positive (negative) amplitude. The outer contour gives the classical turning point. The radial coordinates are mass weighted so that $\tilde{r}_1 = \alpha r_1$ and $\tilde{r}_2 = r_2/\alpha$ where $\alpha = (3/4)^{1/4}$.

ever it was also found that the volume of phase space occupied was small. Two-dimensional quantum-mechanical calculations[24,27] have since confirmed the presence of the states, but this is the first time the states have been observed in a full 3D calculation.

It has been suggested that the course-grained regularity observable in the Carrington and Kennedy spectrum of H_3^+ can be explained in terms of these horseshoe states.[28] The present calculations do not probe high enough energy regions to comment on this directly. However, by combining these quantum calculations with classical calculations extending to above dissociation, considerable insight may be obtained. This will be the subject of a future publication.[29]

In the course of their 2D study of H_3^+, TBP (Ref. 24) identified some periodic orbits in the high-energy regime that had not been previously observed. Although these orbits were found to be largely unstable in 3D, it is interesting to note that quantum states with this nature persist in our 3D calculations; see Fig. 1, state 99. These states are described as being inverted hyperspherical modes in Table II.

Table III shows that the convergence of the rotational portion of our calculation is very good and consistently better than for the corresponding vibrational levels. Therefore the occurrence of relatively large splittings in the degeneracies of a number of states was somewhat surprising. The comparison with the earlier FBR results suggest one possible explanation of this phenomenon. Several of our $p = 1$ states are slightly higher than the corresponding values of Miller and Tennyson. For $J = 1$ these results are simply the solutions of $\hat{H}^k$ for $k = 1$. It is possible that these results are not

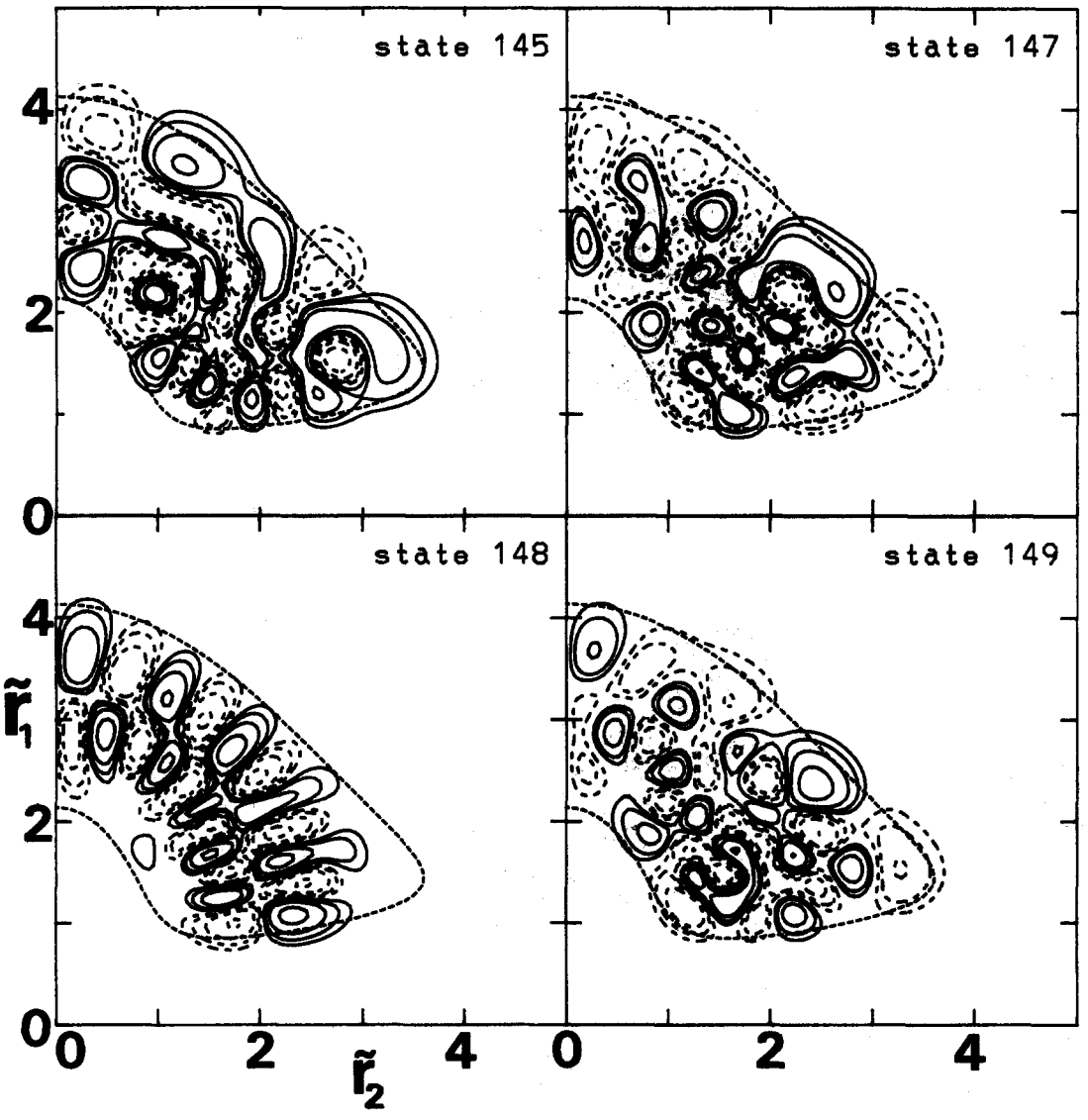

FIG. 2. Cuts through the wave functions of four even $J = 0$ states with $\theta = 90°$. Contours and coordinates as in Fig. 1.

as well converged as the corresponding $k = 0$ ones and that this problem is worse for linear geometries. We note that Tennyson and Sutcliffe[30] had to use different spherical oscillator functions for their $J = 0$ and $J = 1$ calculations on the quasilinear CH_2^+ molecule to circumvent this problem.

Analysis of the $J = 1 \leftarrow 0$ excitation of the highly-excited bending or horseshoe states shows a rapid increase, particularly for the $J = 1, p = 1$ state. Such an increase is characteristic of the change from a bent to a quasilinear molecule.[30] As such, the horseshoe states can be thought of as the large-amplitude bending modes of a quasilinear H_3^+.

V. CONCLUSIONS

We have developed a discrete variable method for the study of rovibrational states of triatomic systems. This method is an extension of the earlier work of Bačić and Light,[6,10] employing a two-step variational method[14] to treat rotationally excited states. For AB_2 systems, symmetrization of the DVR means that the second symmetry can be computed at little extra computational cost.

This method has been applied to H_3^+ yielding energies for the lowest 180 vibrational states of the system, covering two-thirds of the way to the dissociation limit. The range encompasses the entire range of validity of the accurate potential-energy surface employed, demonstrating the urgent need for a global surface for this challenging system if detailed studies of the near-dissociation region are to be undertaken.

ACKNOWLEDGMENTS

We wish to thank Brian Sutcliffe for several helpful discussions and the staff of the Weizmann Institute Computer Centre on whose Convex 200 machine these calculations were performed.

[1] J. Tennyson, Comput. Phys. Rep. **4**, 1 (1986).
[2] S. Carter and N. C. Handy, Comput. Phys. Rep. **5**, 117 (1986).
[3] P. Jensen, J. Mol. Spectrosc. **128**, 478 (1988).
[4] J. Tennyson and S. Miller, Comput. Phys. Commun. (in press).
[5] S. Carter, P. Rosmus, N. C. Handy, S. Miller, J. Tennyson, and B. T. Sutcliffe, Comput. Phys. Commun. (in press).
[6] Z. Bačić and J. C. Light, J. Chem. Phys. **85**, 4594 (1986); **86**, 3065 (1987).

[7]Z. Bačić, D. Watt, and J. C. Light, J. Chem. Phys. **89**, 947 (1988).
[8]R. M. Whitnell and J. C. Light, J. Chem. Phys. **89**, 3674 (1988).
[9]R. M. Whitnell and J. C. Light, J. Chem. Phys. **90**, 1774 (1989).
[10]Z. Bačić and J. C. Light, Ann. Rev. Phys. Chem. (in press).
[11]A. Carrington and R. A. Kennedy, J. Chem. Phys. **81**, 91 (1984).
[12]J. Tennyson and B. T. Sutcliffe, J. Chem. Phys. **77**, 4061 (1982); **79**, 43 (1983).
[13]B. T. Sutcliffe and J. Tennyson, Mol. Phys. **58**, 1053 (1986).
[14]J. Tennyson and B. T. Sutcliffe, Mol. Phys. **58**, 1067 (1986).
[15]W. Meyer, P. Botschwina, and P. G. Burton, J. Chem. Phys. **84**, 891 (1986).
[16]S. Miller and J. Tennyson, J. Mol. Spectrosc. **128**, 183 (1987).
[17]S. Miller and J. Tennyson, J. Mol. Spectrosc. **128**, 530 (1988); **133**, 237 (1989).
[18]S. Miller and J. Tennyson, J. Mol. Spectrosc. (in press).
[19]K. Evenson and C. Demuynck (private communication).
[20]P. Drossart, J.-P. Maillard, J. Caldwell, S. J. Kim, J. K. G. Watson, M. A. Majewski, J. Tennyson, S. Miller, S. Atreya, J. Clarke, J. H. Waite, Jr., and R. Wagener, Nature (London) **340**, 539 (1989).
[21]E. U. Condon and G. H. Shortley *The Theory of Atomic Spectra* (Cambridge University, Cambridge, 1935).
[22]A. S. Dickinson and P. R. Certain, J. Chem. Phys. **49**, 4204 (1968).
[23]B. T. Sutcliffe, S. Miller, and J. Tennyson, Comput. Phys. Commun. **51**, 73 (1986).
[24]J. Tennyson, O. Brass, and E. Pollak, J. Chem. Phys. (submitted).
[25]J. K. G. Watson, J. Mol. Spectrosc. **103**, 350 (1984).
[26]M. Berblinger, E. Pollak, and Ch. Schlier, J. Chem. Phys. **88**, 5643 (1988).
[27]J. M. Gomez Llorrente, J. Zakrzewski, H. S. Taylor, and K. C. Kulander, J. Chem. Phys. **90**, 1505 (1989).
[28]J. M. Gomez Llorrente and E. Pollak, J. Chem. Phys. **89**, 1195 (1988); **90**, 5406 (1989).
[29]O. Brass, J. Tennyson, and E. Pollak, J. Chem. Phys. (submitted).
[30]J. Tennyson and B. T. Sutcliffe, J. Mol. Spectrosc. **101**, 71 (1983).